Langmuir

ARTICLE

pubs.acs.org/Langmuir

Electrochemical Stability of Self-Assembled Alkylphosphate Monolayers on Conducting Metal Oxides

Oktay Yildirim,[†,‡] M. Deniz Yilmaz,[‡] David N. Reinhoudt,[‡] Dave H. A. Blank,[†] Guus Rijnders,[*,†] and Jurriaan Huskens[*,‡]

[†]Inorganic Materials Science and [‡]Molecular Nanofabrication Group, MESA+ Institute for Nanotechnology, University of Twente, P.O. Box 217, 7500 AE, Enschede, The Netherlands

ABSTRACT: Alkylphosphate self-assembled monolayers (SAMs) were prepared on Nb-doped $SrTiO_3$ (Nb−STO) conducting metal oxide substrates. Unlike thiols on gold, the alkylphosphate SAMs on Nb−STO exhibited an electrochemical stability over a wide voltage range from −2 to 2 V. Cyclic voltammetry showed that the SAM modification inhibited the electrochemical activity of the underlying conducting substrate with an efficiency dependent on the chain length. Impedance spectroscopy showed that SAM-modified Nb−STO substrates have a significantly higher resistance than bare substrates.

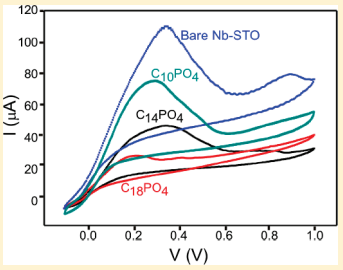

INTRODUCTION

There has been vast interest into self-assembled monolayers (SAMs) owing to their ease of preparation, precise control of structure at a molecular level, and wide variety of functionalities allowing a versatile manipulation of surface and interface properties.[1−4] Electrochemical techniques such as electrochemical impedance spectroscopy (EIS) and cyclic voltammetry (CV) are widely used to observe the properties of SAM-modified electrode surfaces,[5−7] usually by comparing it with the bare electrode.[4,7−10] SAMs reduce the electrochemical activity of the surface by forming effective insulating barriers to electron transfer and ion penetration.[4,6−14]

Similar to SAMs of thiols on gold and silanes on SiO_2,[15,16] there has been a substantial number of studies on SAMs on metal oxides.[17−34] Alkylphosphates and alkylphosphonates form SAMs with very high ambient stability on metal oxides such as Ta_2O_5, Al_2O_3, ZrO_2, and TiO_2 without the need for controlled environmental conditions,[25,30,31,34−39] but they are known to be unstable in aqueous conditions.[30,38]

Most of the electrochemical studies on SAMs involve thiols on gold.[3,6,40] However, upon repetitive CV cycles or by extending the operational potential windows during CV, thiol molecules desorb from the surface, leading to destruction of the monolayer.[3,11,41−44] Octadecyltrichlorosilane monolayers on gold have been reported to be electrochemically unstable as well.[1] The need for capture probe immobilization within FET biosensors based on Ta_2O_5[45] sets a good example where stable monolayers on metal oxide surfaces are crucial. There are few studies about alkylphosphonates in electrochemistry, such as on nitinol[7] or on ITO,[4] in which case they were studied within a rather narrow potential range from −0.5 to 1 V.

Here, the electrochemical behavior and stability of alkylphosphate SAMs with different chain lengths assembled on conducting metal oxide Nb-doped $SrTiO_3$ (Nb−STO) is investigated by using CV and EIS.

EXPERIMENTAL SECTION

Materials. Polished substrates of (100) 0.5 wt % niobium-doped $SrTiO_3$ (Nb−STO) (1 × 10 × 10 mm) were purchased from SurfaceNet GmbH, Germany. These substrates were cut into 5 × 5 mm^2 pieces with a diamond saw and cleaned by ultrasonication in acetone and ethanol for 30 min each. Decylphosphoric acid (DP), tetradecylphosphoric acid (TDP), and octadecylphosphoric acid (ODP) were supplied by A. Wagenaar and J. Engbersen (RUG, Groningen).

SAM Formation. Oxygen plasma-cleaned Nb−STO substrates were immersed into 0.125 mM alkyl phosphoric acid solutions in 100:1 v/v hexane:isopropanol for 2 days at room temperature. Afterward, the samples were rinsed with the pure solvent mixture and dried under a flow of N_2.

Measurements. *Electrochemistry.* Cyclic voltammetry (CV) measurements were performed with an AUTOLAB PGSTAT10 at 100−200 mV/s scan rates in a voltage range from −2 to 2 V. Measurements were performed on bare or SAM-modified Nb−STO in 0.1 M tetrabutylammonium hexafluorophosphate ($Bu_4N^+PF_6^-$) in acetonitrile using Ag/AgCl and Pt as the reference and counter electrodes, respectively. All scans shown are averages over five measurements. Electrochemical impedance measurements were performed in the same setup within the range from 10 kHz to 10 mHz at −0.2 V.

X-ray Photoelectron Spectroscopy (XPS). Elemental composition was analyzed by a Physical Electronics Quantera Scanning X-ray Multiprobe instrument, equipped with a monochromatic Al Kα X-ray source operated at 1486.7 eV and 25 W. Spectra were referenced to the main C1s peak at 284.80 eV.

Scanning Tunneling Microscopy (STM). The morphology of SAM-modified Nb−STO was observed by an easyScan 2 STM at ambient and room temperature.

Received: March 11, 2011
Revised: July 7, 2011
Published: July 11, 2011

Contact Angle (CA). Measurements were done with a Kruss G10 goniometer equipped with a CCD camera. Contact angles were determined automatically during growth of the droplet by a drop shape analysis. Milli-Q water (18.4 MOhm.cm) was used as a probe liquid.

RESULTS AND DISCUSSION

SAM Formation. Previously, we have shown the detailed characterization of a tetradecylphosphate (TDP) SAM on alumina, which resulted in successful formation of a homogeneous SAM with high coverage.[34] The height of the TDP layer was around 1.5 nm. This is somewhat lower than the extended adsorbate length (2 nm), which indicates a tilt in the SAM layer similar to various alkyl phosph(on)ate SAMs on metal oxides[25,31,34,35]

Preparation of monolayer-modified Nb−STO substrates was performed according to literature procedures.[25,30,31,34,35] Clean Nb−STO substrates were immersed into alkylphosphate (with 10 (DP), 14 (TDP), 18 (ODP) C atoms) solutions for 2 days at room temperature, rinsed afterward with solvent, and dried under a flow of N_2 to yield an alkyl-functionalized substrate.

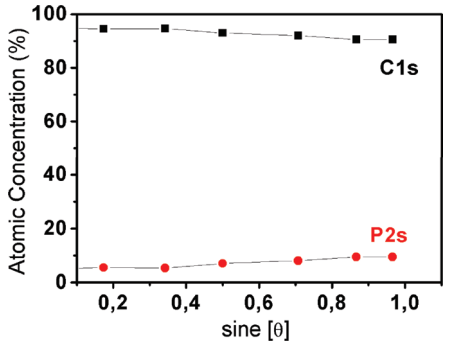

Figure 1. Angle-dependent XPS of TDP SAM-covered Nb-doped $SrTiO_3$.

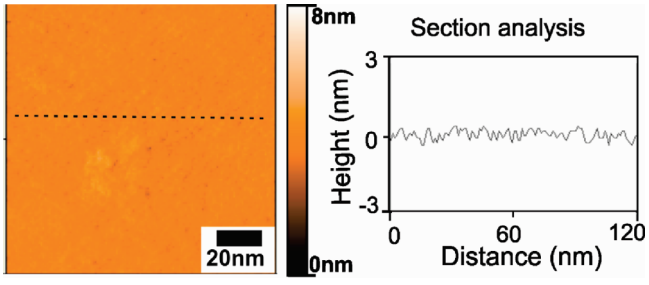

Figure 2. Scanning tunneling micrograph of a TDP-covered Nb−STO surface with section analysis.

As a representative example of the whole series, TDP SAMs were characterized extensively. The water contact angle (CA) of oxygen plasma-cleaned Nb−STO was below 10°, which increased to 115° after TDP SAM modification. The high CA value indicates a quite hydrophobic surface, and this confirms a methyl-terminated SAM. XPS measurements on TDP-modified Nb−STO showed that all the expected elements were present on the surface in the expected ratios. To observe the orientation of the TDP molecules, angle-dependent XPS was performed (Figure 1). The electron takeoff angles were varied between 5° and 90°. The results show a clear dependence of the elemental peak intensities on the detection angle. As the detection angle increases, the amount of C_{1s} from the alkyl chain decreases and the contribution of P_{2s} from the headgroup increases. This indicates that P is located in the inner part of the SAM which is closer to the substrate surface when compared to C.[31,34] The result is in line with the CA value, which suggests a tails-up orientation, and agrees with literature, since alkyl phosphates and alkyl phosphonates were reported to bind metal oxides through the phosph(on)ate headgroup.[31,34,35,46]

STM on TDP-covered Nb−STO showed that the SAM is smooth and continuous (Figure 2). Model calculations performed according to a literature procedure[47] showed that the SAM was homogeneous with a thickness of 1.7 nm.

Contact angles of DP and ODP SAMs on Nb−STO were identical to the value for the TDP SAM. Moreover, XPS analysis showed very similar elemental compositions, but the angle dependence was not further investigated. Overall, the binding modes for DP and ODP were assumed to be similar to TDP.

Electrochemistry. Cyclic voltammetry (CV) was performed on bare and alkylphosphate (DP, TDP, ODP) modified Nb−STO substrates. The samples were placed in a 0.1 M tetrabutylammonium hexafluorophosphate ($Bu_4N^+PF_6^-$) solution in acetonitrile, and data were collected with 100−200 mV/s scan rates within potential ranges from either −0.1 to 1 V or −2 to 2 V. All recorded data are averages of five scans.

Figure 3 shows CVs performed on bare and TDP-modified Nb−STO substrates within the range from −0.1 to 1 V. The clearly visible oxidation peak can potentially be attributed to oxidation of Nb atoms at or close to the surface but was not investigated further. Rather, the redox signal, and the suppression

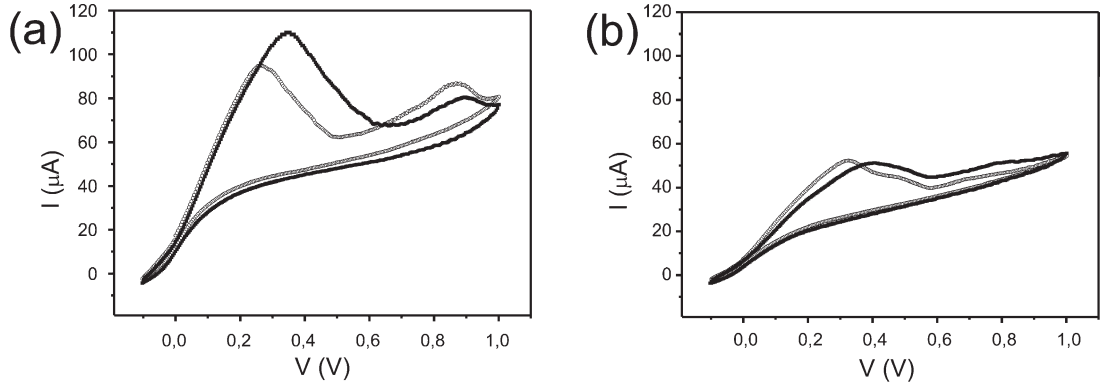

Figure 3. Cyclic voltammograms on (a) bare and (b) TDP SAM-modified Nb−STO performed at 100 (○) and 200 mV/s (■) scan rates.

dx.doi.org/10.1021/la200925v |*Langmuir* 2011, 27, 9890–9894

thereof, was used as a signature to investigate the blocking effect of an adsorbed, redox-inactive monolayer. Since not much difference was seen between scan rates of 100 and 200 mV/s, the latter was used in further experiments. More importantly, the comparison between the bare and the TDP-covered substrates shows a clear blocking effect of the SAM.

To check the electrochemical stability of a TDP SAM on Nb−STO, the sample was subjected to CV between −0.1 and 1 V, then the potential window was widened from −2 to 2 V, and another measurement was done. Finally, the sample was measured again at the initial potential window (from −0.1 to 1 V). The scans shown (Figure 4) are averages of five scans, and the total duration of the experiment was 45 min. There was no noticeable difference between the scans performed at the same potential range, which confirms the stability of the monolayer. More importantly, as seen in Figure 4, the first and third measurements are identical, which means that the TDP SAM on Nb−STO is stable over a voltage range of as wide as from −2 to 2 V. There appears to be no noticeable change, damage, or desorption of the SAM. This marks a clear contrast with thiols on gold, which have a rather limited potential window at which they are stable.[44] In the case of thiols, oxidation and reduction processes occur at the thiol headgroups of the adsorbates, thus diminishing their affinity for the gold surface and leading to concomitant desorption. The here observed high electrochemical stability of the phosphate SAMs on Nb−STO may be due to the nature of the bond between the phosphate headgroup and the metal oxide surface and potentially to the absence of oxidative and reductive desorption pathways.

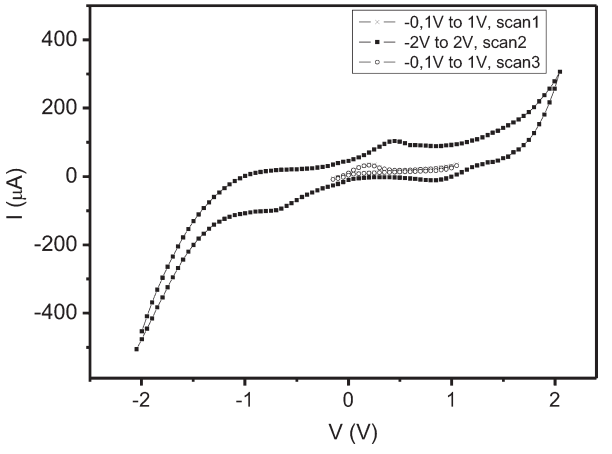

Figure 4. Series of cyclic voltammograms of TDP SAM-modified Nb−STO performed from −0.1 to 1 V ("scan1") and back, then from −2 to 2 V ("scan2") and back, followed by another experiment from −0.1 to 1 V (scan 3), all at a scan rate of 200 mV/s. Each experimental series shown here represents an average over 5 scans.

Figure 5 shows a comparison of the CVs of a bare substrate and substrates modified with alkylphosphate SAMs of different chain lengths. The CVs of bare and modified Nb−STO have similar shapes, showing a single oxidative peak around 0.3 V, but with reduced height for the SAM-modified samples. Since the samples were scanned five times each, with no apparent change to the shape and height of the CV graph, SAMs are stable and resistant to oxidative desorption.[7] The ODP SAM blocks the electrochemical activity of the substrate and effectively insulates it from the environment; however, there is still significant activity for DP and TDP, which may be due to more pinhole defects compared to the longer SAMs. The longer chain alkylphosphates seem to be more efficient compared to shorter ones, and the current has a monotonic dependence on chain length (Figure 5b).

Electrochemical impedance spectroscopy (EIS) was performed in the range from 10 kHz to 10 mHz at a potential of −0.2 V. Bare Nb−STO and DP- and TDP-modified Nb−STO were compared. EIS provides a measure of the resistance and quality of the coating on a conducting substrate.[7] Figure 6 shows the impedance data, represented as Bode and Nyquist plots, of bare and DP- and TDP-modified Nb−STO substrates. Full modeling of the EIS data to an equivalent circuit was not attempted here. Nevertheless, the data support that the resistances follow the trend $R_{bare} < R_{DP} < R_{TDP}$. As seen in the Nyquist plot, the impedance semicircle of TDP is larger than that of DP, which indicates that TDP has a higher resistance (∼100 vs ∼50 kΩ) and forms a better barrier in insulating the conducting metal oxide. This is expected since TDP has a longer chain length. The capacitance values can be estimated as 5.5×10^{-7} and 3.7×10^{-7} F for DP and TDP, respectively.

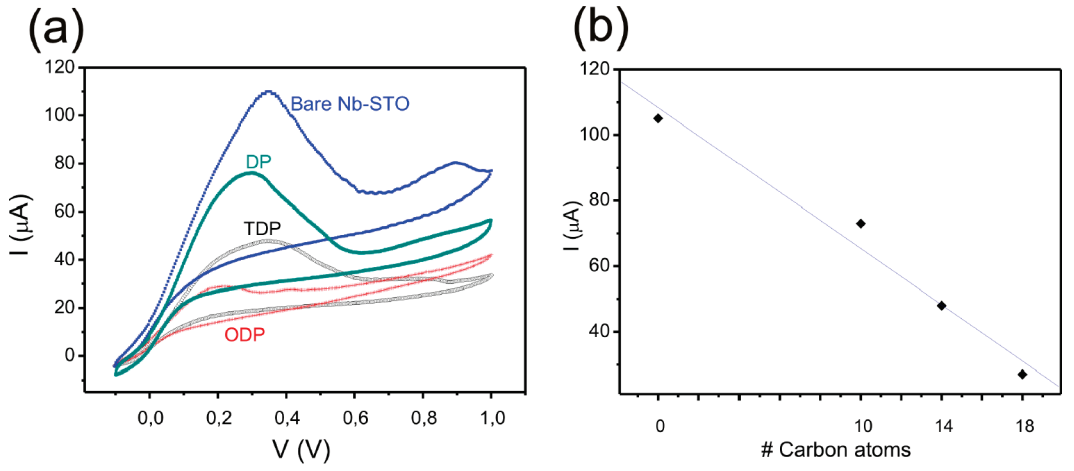

Figure 5. (a) Cyclic voltammograms of bare and alkylphosphate SAM-modified Nb−STO substrates. (b) Current at 0.3 V vs alkyl chain length. The linear fit is a guide to the eye, not a result of a model.

dx.doi.org/10.1021/la200925v |*Langmuir* 2011, 27, 9890–9894

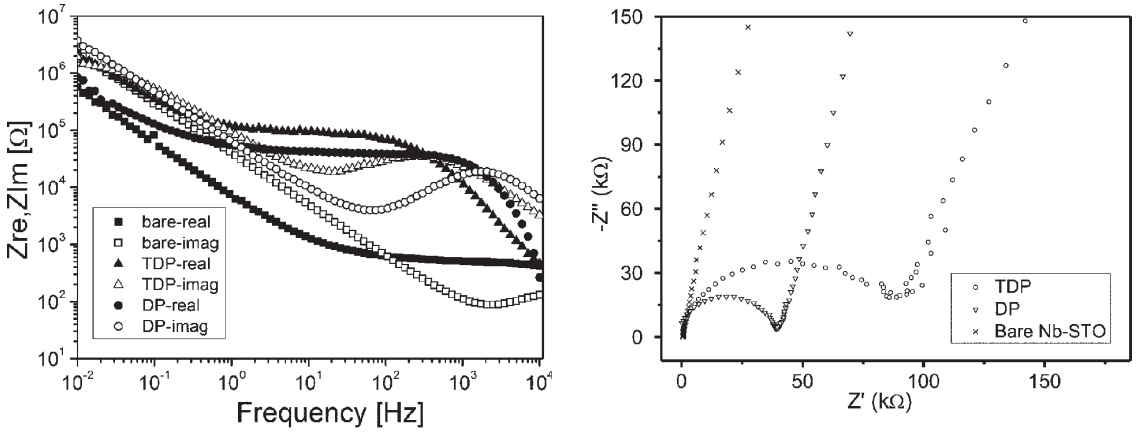

Figure 6. Impedance spectroscopy data, represented as Bode (left) and Nyquist (right) plots, of bare and DP and TDP-modified Nb−STO substrates.

CONCLUSIONS

Electrochemistry (CV and EIS) has shown that alkylphosphate SAMs inhibit the electrochemical activity of the Nb−STO conducting metal oxide substrate. The inhibition efficiency increased with increasing chain length of the SAM. Unlike thiols on gold, the alkylphosphate SAMs on Nb−STO show electrochemical stability over a voltage range as wide as from −2 to 2 V. At the same time, this electrochemical stability (in organic solvents) contrasts the limited chemical stability of the monolayers under aqueous conditions. The resistance of a SAM layer is much higher than of the bare substrate and increases with chain length. The described system opens new possibilities to study electrochemical properties of semiconductors functionalized with various phosphate-based adsorbates.

AUTHOR INFORMATION

Corresponding Author

*E-mail: a.j.h.m.rijnders@utwente.nl (G.R.); j.huskens@utwente.nl (J.H.).

ACKNOWLEDGMENT

The authors gratefully acknowledge financial support from the MESA+ Institute for Nanotechnology (SRO Nanofabrication), NanoNed, the Nanotechnology network in The Netherlands, and the Council for Chemical Sciences of The Netherlands Organization for Scientific Research (NWO-CW; grant 700.55.029 to J.H.). We acknowledge Gerard Kip for XPS measurements and Cees van der Marel (Philips Innovation Services) for model calculations on SAMs. We thank A. Wagenaar and J. Engbersen (RUG, Groningen) for providing the alkylphosphates.

REFERENCES

(1) Finklea, H. O.; Robinson, L. R.; Blackburn, A.; Richter, B.; Allara, D.; Bright, T. *Langmuir* **1986**, *2*, 239–244.
(2) Sabatani, E.; Rubinstein, I. *J. Phys. Chem.* **1987**, *91*, 6663–6669.
(3) Shervedani, R. K.; Hatefi-Mehrjardi, A.; Babadi, M. K. *Electrochim. Acta* **2007**, *52*, 7051–7060.
(4) Jedaa, A.; Burkhardt, M.; Zschieschang, U.; Klauk, H.; Habich, D.; Schmid, G.; Halik, M. *Org. Electron.* **2009**, *10*, 1442–1447.
(5) Campuzano, S.; Pedrero, M.; Montemayor, C.; Fatas, E.; Pingarron, J. M. *J. Electroanal. Chem.* **2006**, *586*, 112–121.
(6) Ganesh, V.; Pal, S. K.; Kumar, S.; Lakshminarayanan, V. *J. Colloid Interface Sci.* **2006**, *296*, 195–203.
(7) Quinones, R.; Gawalt, E. S. *Langmuir* **2008**, *24*, 10858–10864.
(8) Diao, P.; Jiang, D. L.; Cui, X. L.; Gu, D. P.; Tong, R. T.; Zhong, B. *J. Electroanal. Chem.* **1999**, *464*, 61–67.
(9) Finklea, H. O.; Snider, D. A.; Fedyk, J. *Langmuir* **1990**, *6*, 371–376.
(10) Porter, M. D.; Bright, T. B.; Allara, D. L.; Chidsey, C. E. D. *J. Am. Chem. Soc.* **1987**, *109*, 3559–3568.
(11) Finklea, H. O.; Avery, S.; Lynch, M.; Furtsch, T. *Langmuir* **1987**, *3*, 409–413.
(12) Janek, R. P.; Fawcett, W. R.; Ulman, A. *Langmuir* **1998**, *14*, 3011–3018.
(13) Ma, H. Y.; Yang, C.; Chen, S. H.; Jiao, Y. L.; Huang, S. X.; Li, D. G.; Luo, J. L. *Electrochim. Acta* **2003**, *48*, 4277–4289.
(14) Rubinstein, I.; Steinberg, S.; Tor, Y.; Shanzer, A.; Sagiv, J. *Nature* **1988**, *332*, 426–429.
(15) Onclin, S.; Ravoo, B. J.; Reinhoudt, D. N. *Angew. Chem., Int. Ed.* **2005**, *44*, 6282–6304.
(16) Schreiber, F. *Prog. Surf. Sci.* **2000**, *65*, 151–256.
(17) Acton, B. O.; Ting, G. G.; Shamberger, P. J.; Ohuchi, F. S.; Ma, H.; Jen, A. K. Y. *ACS Appl. Mater. Interf.* **2010**, *2*, 511–520.
(18) Adadi, R.; Zorn, G.; Brener, R.; Gotman, I.; Gutmanas, E. Y.; Sukenik, C. N. *Thin Solid Films* **2010**, *518*, 1966–1972.
(19) Allara, D. L.; Nuzzo, R. G. *Langmuir* **1985**, *1*, 45–52.
(20) Allara, D. L.; Nuzzo, R. G. *Langmuir* **1985**, *1*, 52–66.
(21) Amalric, J.; Mutin, P. H.; Guerrero, G.; Ponche, A.; Sotto, A.; Lavigne, J. P. *J. Mater. Chem.* **2009**, *19*, 141–149.
(22) Bozzini, S.; Petrini, P.; Tanzi, M. C.; Zurcher, S.; Tosatti, S. *Langmuir* **2010**, *26*, 6529–6534.
(23) Klauk, H.; Zschieschang, U.; Pflaum, J.; Halik, M. *Nature* **2007**, *445*, 745–748.
(24) Kropman, B. L.; Blank, D. H. A.; Rogalla, H. *Langmuir* **2000**, *16*, 1469–1472.
(25) Messerschmidt, C.; Schwartz, D. K. *Langmuir* **2001**, *17*, 462–467.
(26) Mitchon, L. N.; White, J. M. *Langmuir* **2006**, *22*, 6549–6554.
(27) Paramonov, P. B.; Paniagua, S. A.; Hotchkiss, P. J.; Jones, S. C.; Armstrong, N. R.; Marder, S. R.; Bredas, J. L. *Chem. Mater.* **2008**, *20*, 5131–5133.
(28) Paszternak, A.; Felhosi, I.; Paszti, Z.; Kuzmann, E.; Vertes, A.; Kalman, E.; Nyikos, L. *Electrochim. Acta* **2010**, *55*, 804–812.
(29) Sekitani, T.; Yokota, T.; Zschieschang, U.; Klauk, H.; Bauer, S.; Takeuchi, K.; Takamiya, M.; Sakurai, T.; Someya, T. *Science* **2009**, *326*, 1516–1519.
(30) Sun, S. Q.; Leggett, G. J. *Nano Lett.* **2007**, *7*, 3753–3758.
(31) Textor, M.; Ruiz, L.; Hofer, R.; Rossi, A.; Feldman, K.; Hahner, G.; Spencer, N. D. *Langmuir* **2000**, *16*, 3257–3271.
(32) Wang, D. H.; Ni, Y. H.; Huo, Q.; Tallman, D. E. *Thin Solid Films* **2005**, *471*, 177–185.
(33) Yasseri, A. A.; Kobayashi, N. P.; Kamins, T. I. *Appl. Phys. A: Mater.* **2006**, *84*, 1–5.

(34) Yildirim, O.; Gang, T.; Kinge, S.; Reinhoudt, D. N.; Blank, D. H. A.; van der Wiel, W. G.; Rijnders, G.; Huskens, J. *Int. J. Mol. Sci.* **2010**, *11*, 1162–1179.
(35) Gawalt, E. S.; Avaltroni, M. J.; Koch, N.; Schwartz, J. *Langmuir* **2001**, *17*, 5736–5738.
(36) Gnauck, M.; Jaehne, E.; Blaettler, T.; Tosatti, S.; Textor, M.; Adler, H. J. P. *Langmuir* **2007**, *23*, 377–381.
(37) Hahner, G.; Hofer, R.; Klingenfuss, I. *Langmuir* **2001**, *17*, 7047–7052.
(38) Liakos, I. L.; Newman, R. C.; McAlpine, E.; Alexander, M. R. *Langmuir* **2007**, *23*, 995–999.
(39) Pawsey, S.; Yach, K.; Reven, L. *Langmuir* **2002**, *18*, 5205–5212.
(40) Mekhalif, Z.; Riga, J.; Pireaux, J. J.; Delhalle, J. *Langmuir* **1997**, *13*, 2285–2290.
(41) Hobara, D.; Ota, M.; Imabayashi, S.; Niki, K.; Kakiuchi, T. *J. Electroanal. Chem.* **1998**, *444*, 113–119.
(42) Schneider, T. W.; Buttry, D. A. *J. Am. Chem. Soc.* **1993**, *115*, 12391–12397.
(43) Walczak, M. M.; Popenoe, D. D.; Deinhammer, R. S.; Lamp, B. D.; Chung, C. K.; Porter, M. D. *Langmuir* **1991**, *7*, 2687–2693.
(44) Beulen, M. W. J.; Kastenberg, M. I.; van Veggel, F.; Reinhoudt, D. N. *Langmuir* **1998**, *14*, 7463–7467.
(45) Goykhman, I.; Korbakov, N.; Bartic, C.; Borghs, G.; Spira, M. E.; Shappir, J.; Yitzchaik, S. *J. Am. Chem. Soc.* **2009**, *131*, 4788–4794.
(46) Spori, D. M.; Venkataraman, N. V.; Tosatti, S. G. P.; Durmaz, F.; Spencer, N. D.; Zurcher, S. *Langmuir* **2007**, *23*, 8053–8060.
(47) van der Marel, C.; Yildirim, M.; Stapert, H. R. *J. Vac. Sci. Technol. A* **2005**, *23*, 1456–1470.